Prediction of Hourly Solar Radiation on Horizontal and Inclined Surfaces for Muscat/Oman

N.Z. Al-Rawahi*, Y.H. Zurigat and N.A. Al-Azri

Department of Mechanical and Industrial Engineering, College of Engineering, Sultan Qaboos University, P.O. Box 33, Postal Code 123, Al Khoud, Muscat, Oman

التنبؤ بالإشعاع الشمسي لكل ساعة على الأسطح الأفقية والمائلة في مسقط/سلطنة عمان

ن. ز. الرواحي*، ي. ح. زريقات و ن. أ. العزري

الخلاصة: تم استخدام نماذج حسابية في هذه الورقة لإيجاد الإشعاعات الشمسية المباشرة والمنعكسة من طبقات الجو على الأسطح الأرضية لكل ساعة بناءً على الإشعاع الشمسي الكلي اليومي على سطح أفقي، بالإضافة إلى ذلك فقد تم استخدام نماذج حسابية لحساب هذه الإشعاعات للأسطح المائلة. إن معظم المقادير التي تم استخدام النماذج الحسابية لإيجادها في هذا العمل مطلوبة كبيانات أولية في عدة برمجيات للمحاكاة الحرارية للمباني ولمحاكاة أنظمة الطاقة الشمسية. تم عرض ومناقشة اتجاهات عامة مهمة للتغيرات التي تحدث لمقدار الإشعاع الشمسي الساقط على سطح مائل مع تغير الوقت واتجاه السطح. عندما قورنت نتائج هذا البحث ببعض القياسات الميدانية فقد وجد هناك توافق ممتاز بينهما. تم عرض تأثير اتجاه ودرجة ميلان السطح على الإشعاع الشمسي الساقط على سطح مائل وأيضا الاتجاه ودرجة الميلان المثلي لضمان الحد الأقصى للإشعاع الشمسي الساقط على الأسطح المائلة في مسقط. إن النتائج المعروضة في هذه الورقة مفيدة لاستخدامها في الحصول على تقديرات سريعة للإشعاعات الشمسية واستخدامها في حساب طاقة التبريد للمباني وأداء مستقبلات الطاقة الشمسية. بالإضافة إلى ذلك فإن النماذج الحسابية وبرنامج الحاسوب التي تم تطويره في هذا العمل يمكن استخدامها كأساس لأي برنامج حاسوبي للتصميم الحراري للمباني ولحسابات تصميم أنظمة الطاقة الشمسية.

المفردات المفتاحية: الإشعاعات الشمسية، التبريد بالطاقة الشمسية، مستقبلات الطاقة الشمسية

Abstract: In this paper, hourly terrestrial radiation: direct beam, diffuse and global solar radiation are modelled and calculated based on daily measured data for a horizontal surface. In addition, the same parameters were modelled for inclined surfaces. Most of the parameters modelled in this work represent a part of the input data required by building thermal simulation and solar energy systems software. Important trends of the solar radiation on tilted surfaces as a function of time and direction are being presented and discussed. The comparison of some of the results with measured data from other sources shows good agreement. The effect of tilt angle and orientation on the incident solar radiation fluxes are presented along with optimum surface tilt angles and directions for maximum solar radiation collection in Muscat area. The results presented in this paper are quite useful for quick estimation of solar radiation for calculations of cooling load and solar collector performance. Also, the models and the computer code developed in this work form the backbone of any computer-aided building thermal design and solar systems design calculations.

Keywords: Solar radiation, Solar cooling, Solar collectors

1. Introduction

Building transient thermal simulation software programs such as TRNSYS require hourly weather parameters in standard Typical Meteorological Year format (TMY2, for example). Each line of the TMY2 record has a total of 70 parameters and indices that need to be specified based on measured data or calculated from measured data or estimated. Some of the important elements that normally are not measured are

the hourly terrestrial solar radiation fluxes on horizontal surfaces. Terrestrial solar radiation; direct beam, diffuse and global hourly solar fluxes are modelled and calculated based on average daily measured data. Other data such as dew point and wet bulb temperatures are also calculated based on the measured dry bulb and relative humidity data. The design of building conventional HVAC systems requires cooling load calculations which are based on hourly weather data. Also, the design of solar cooling systems requires

---

Correseponding author's e-mail: alrawahi@squ.edu.om

cooling load calculations, collector and thermal energy storage sizing, and performance evaluation under transient conditions. Thus, the need for accurate predictions of hourly solar flux data for a given location is quite obvious.

Solar radiation models are used to predict direct, diffused, and global radiation based on certain known variables. The models can be classified into either parametric or decomposition models. The models in the former category require the knowledge of atmospheric conditions (ASHRAE handbook, 1999; Iqbal 1978; Gueymard 1993). The decomposition models, on the other hand, use the known solar global radiation data (Liu and Jordan 1960; Lam and Li 1996; Badescu 2002). A good comparison between the two types of models can be found in (Wong and Chow 2008) where comparison between representative models from both categories with measured data was presented. Decomposition models use solar global radiation data on horizontal surface to predict the direct and diffuse radiation components. The use of these models is supported by the availability of a large number of locations that keep records of the global radiation on a horizontal surface. The decomposition models can be further classified according to the used method as empirical, analytical, numerical and statistical, and neural networks models (Liu and Jordan 1962; Lam and Li 1996; Tymvios *et al*. 2005; Zervas *et al*. 2008; Ulgen and Hepbasli 2009; Mellit *et al*. 2010).

A number of models were shown to predict the global solar radiation. However, modelling the diffuse solar radiation has been a challenge for researchers. This difficulty in modelling the diffuse radiation component reflects on the ability to have accurate models for the solar radiation on tilted surfaces which is generally calculated using total, direct, and diffuse solar radiation fluxes. The accuracy of models for solar radiation on tilted surfaces is highly affected by the accuracy of the diffuse solar radiation models. The isotropic model of Liu and Jordan (1962) and the anisotropic model of Perez *et al*. (1990) are among the well known models in this field and will be used in this work. In their study, (Padovan and Del Col 2010) compared the predictions of a number of models used to predict diffuse and total radiation on tilted surfaces including the models of (Liu and Jordan 1962; Perez *et al*. 1990). They found that for southern tilted surfaces, the models have similar accuracy but for the western tilted surfaces the anisotropic models, like that of Perez e*t al*. (1990), perform better. This is because, in the northern hemisphere unlike the west-tilted surfaces, the south-tilted surfaces receive more direct solar radiation and less diffuse radiation. They found that the error in the diffuse solar radiation increases the error in estimating radiation on tilted surfaces signifi-

cantly. Similar conclusions were reported by Noorian *et al*. (2008).

In the presented work, decomposition models for the prediction of hourly solar fluxes on horizontal and inclined surfaces have been implemented with detailed description presented in the next sections. These models and the computer code developed in this work form the backbone of any computer-aided building thermal design and solar systems design calculations.

2. Estimation of Hourly Solar Flux Compo-nents

The total hourly solar radiation falling on a horizontal surface, I_{th} in W.h/m^2, could be estimated from the daily global radiation, H (in kJ/m^2 per day) in accordance with (Duffie and Beckman 1984) as follows:

$$I_{th} = \frac{r \cdot H}{3.6} \qquad (1)$$

Here 3.6 is a conversion factor (3.6 W.h/m^2 = kJ/m^2), r is the ratio I_{th} / H and is given by (Collares-Pereira and Rable 1979):

$$r = \frac{\pi}{24} \cdot (a + b.cos(W)) \cdot \left[\frac{cos(W) - cos(Ws)}{sin(Ws) - \frac{\pi}{180} \cdot Ws.cos(Ws)} \right] \qquad (2)$$

$$a = 0.409 + 0.5016 \, sin(Ws - 60) \qquad (3)$$

$$b = 0.6609 + 0.4767 \, sin(Ws - 60) \qquad (4)$$

W is the hour angle of the sun (in degrees) given by:

$$W = \left(\frac{360}{24}\right) \times \left(h - 12.0\right) \qquad (5)$$

h is the time of the day (solar time) in hours and Ws is the sunset hour angle (in degrees), given by:

$$Ws = cos^{-1} \left(-tan(\phi) \, tan(\delta) \right) \qquad (6)$$

ϕ is the location latitude angle (in degrees) and δ is the declination angle of the sun (in degrees) given by:

$$\delta = 23.45 \times sin\left[360 \times \frac{284 + day}{365} \right] \qquad (7)$$

day is the day of the year under consideration (1 to 365).

It should be noted that while the equations involving solar radiation terms use solar time, the different climate data obtained from meteorological stations are normally given in standard time (local time in the

weather station). In addition, the output from the solar radiation calculations needs to be expressed in standard time as it is used in solar thermal systems simulations. It is noted, however, that many published work do not take this time difference into consideration. This could be due to the fact that the difference between the standard time and the solar time is sometimes small. In this work, the difference between solar and standard timings was taken into account. The well established relation between the solar time t_{sol} and standard time t_{std} is given by (Duffie and Beckman, 1984):

$$t_{sol} - t_{std} = 4(L_{st} - L_{loc}) + T \tag{8}$$

where L_{st} is the standard meridian for the local time zone, L_{loc} is the longitude of the weather station, and the parameter T is the equation of time (in minutes) defined as:

$$T = 229.2 \times \begin{bmatrix} 0.000075 + 0.001868\,cos(B) - 0.032077\,sin(B) \\ -0.014615\,cos(2B) - 0.04089\,sin(2B) \end{bmatrix} \tag{9}$$

where B is given by:

$$B = (day - 1)\frac{360}{365} \tag{10}$$

The difference between solar time and standard time over the year for Seeb/Muscat area is shown in Fig. 1. Although the difference is small reaching a maximum of 24 minutes, the data reported by Seeb Meteorological Center based on local standard time data were adjusted to solar time.
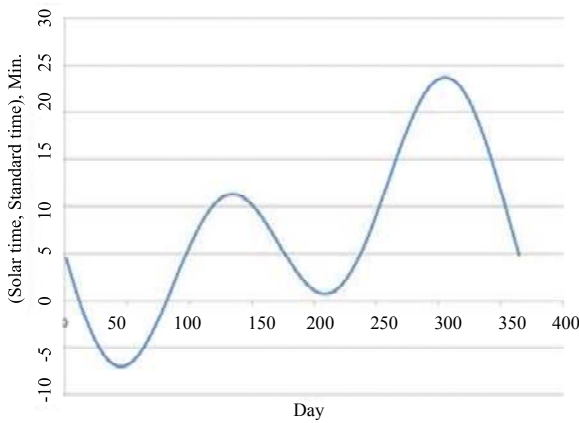

Figure 1. Difference between solar time and standard time over the year for Seeb/Muscat area

The total solar radiation consists of the *direct* or beam radiation coming directly from the solar disc and the *diffuse* component scattered to the ground from the sky dome. The latter depends on the clarity of the sky and could be estimated from the correlation of (Collares-Pereira and Rabl 1979) which gives the daily average diffuse radiation, H_d, as:

$$H_d = H \begin{Bmatrix} 0.775 + 0.00606(Ws - 90) - \\ [0.505 + 0.00455(Ws - 90)]\,cos(115K_T - 103) \end{Bmatrix} \tag{11}$$

Where K_T is the clearness index for the day, defined as the ratio of the daily radiation on a horizontal surface to the daily extraterrestrial radiation (H_o) on that surface, that is:

$$K_T = \frac{H}{H_o} \tag{12}$$

and

$$H_o = \frac{24 \times 3600 \times I_{sc}}{\pi}\left[\left(1 + 0.033 \times cos\left(\frac{360 \times day}{365}\right)\right)\right.$$
$$\left. \left(cos\phi \times cos\delta \times sinWs + \frac{\pi \times Ws}{180}sin\phi \times sin\delta\right)\right] \tag{13}$$

I_{sc} is the solar constant = 1367 W/m².

The hourly values of the diffuse solar radiation can be estimated from the equation by (Liu and Jordan 1960) which gives:

$$I_d = H_d \frac{24}{\pi} \frac{cos(W) - cos(Ws)}{sin(Ws) - \frac{\pi Ws}{180}cos(Ws)} \tag{14}$$

The direct (beam) component of the solar radiation on a horizontal surface is then obtained from:

$$I_{bh} = I_{th} - I_d \tag{15}$$

The hourly value of the direct solar radiation on a surface normal to the direction of the beam, I_{bn} (important in the design of sun-tracking solar collector systems), can be calculated from:

$$I_{bn} = \frac{I_{bh}}{cos\,\theta_z} \tag{16}$$

Where θ_s is the solar zenith angle calculated by (Duffie and Beckman 1984) as:

$$cos\,\theta_z = cos\phi\,cos\delta\,cosW + sin\phi\,sin\delta \tag{17}$$

The above procedure was used by Al-Hinai and Al-Alawi (1995) for developing Typical Solar Radiation Data for Oman.

3. Estimation of Extraterrestrial Radiation Components

The extraterrestrial radiation on a plane normal to the sun rays is a function of the distance between the

earth and the sun and is given by Duffie and Beckman (1984):

$$E_n = I_{SC}\left(1 + 0.033\cos\left(\frac{360 \times day}{365}\right)\right) \quad (18)$$

Using the solar zenith angle, the extraterrestrial radiation on a horizontal plane can be calculated from:

$$E_h = E_n \times cos(\theta_z) \quad (19)$$

Combining Eqs. (17) and (19), we get the extraterrestrial radiation on a horizontal plane at any hour angle, W as:

$$E_h = I_{SC}\left(1 + 0.033 \times \cos\left(\frac{360 \times day}{365}\right)\right)$$
$$\times \{cos(\phi)cos(\delta)cos(W) + sin(\phi)sin(\delta)\} \quad (20)$$

If the total extraterrestrial solar radiation energy incident on a horizontal plane, I_{eh}, over a certain period of time is required, then Eq. (20) is to be integrated from hour angles W_1 to W_2. This results in the following relation:

$$I_{eh} = \frac{12 \times 3600}{\pi} I_{SC}\left(1 + 0.033\cos\left(\frac{360 \times day}{365}\right)\right) \times$$
$$\left(\begin{array}{l}(cos\,\phi\,cos\,\delta)\times(sin\,W_2 - sin\,W_1)\\ + \dfrac{\pi\,(W_2 - W_1)}{180}(sin\,\phi\,sin\,\delta)\end{array}\right) \quad (21)$$

Here, I_{eh} is in J/m². To have I_{eh} in W.h/m² Eq. (21) is to be divided by 3600. On the other hand, the total extraterrestrial radiation on a plane normal to the sun rays over a certain period of time within a certain day is given simply by multiplying Eq. (18) by that time period in seconds. This is because the normal total extraterrestrial radiation is constant over the day.

4. Estimation of Hourly Solar Flux on Inclined Surfaces

The total radiation received by an inclined surface consists of beam, diffuse, and reflected radiation. The reflected radiation here is the radiation reflected from the surrounding ground. Different models for estimating the total solar radiation on inclined surfaces had been proposed and evaluated. Such studies include the work of Noorian *et al.* (2008) who evaluated twelve models, the study by Nijmeh and Mamlook (2000), and that by Notton *et al.* (1996). Most of the presented models in these reviews proved to give good results. The majority of these models use similar terms for the beam and reflected radiation while differ in the method of calculating the diffuse radiation portion.

The general form of total hourly solar radiation energy incident on an inclined surface I_{ti} (in kJ/m²), is given by:

$$I_{ti} = I_{bh} \times R_b + I_{Td} + I_{th} \times \rho_r \frac{(1 - cos(\beta))}{2} \quad (22)$$

where I_{Td} is the diffuse radiation on the tilted surface, β is the angle the surface makes with the horizontal, ρ_r is the surrounding diffuse reflectance for the total solar radiation, and R_b is the hourly geometric factor given by:

$$R_b = \frac{cos(\theta)}{cos(\theta_Z)} \quad (23)$$

Here θ is the incidence angle, the angle between the beam radiation on a surface and the normal to that surface, and it is given by:

$$\begin{aligned}cos(\theta) = {}& sin(\delta) \times sin(\phi) \times cos(\beta) - sin(\delta) \times\\ & cos(\phi) \times sin(\beta) \times cos(\gamma) +\\ & sin(\delta) \times cos(\phi) \times cos(\beta) \times cos(W) +\\ & cos(\delta) \times sin(\phi) \times sin(\beta) \times cos(\gamma) \times cos(W) +\\ & cos(\delta) \times sin(\beta) \times sin(\gamma) \times sin(W)\end{aligned}$$
$$(24)$$

where γ is the surface azimuth angle defined as the deviation of the projection on a horizontal plane of the normal to the surface from the local meridian, with zero due south, east negative, and west positive.

Among the methods available for prediction of radiation fluxes on tilted surfaces is the method of (Liu and Jordan 1962). This is a simple isotropic model that had been tested by many investigators and found to give good results. In this method the diffuse radiation on the tilted surface is given by:

$$I_{Td} = I_d \frac{(1 + cos(\beta))}{2} \quad (25)$$

Another method for the estimation of the diffuse solar radiation is the anisotropic model of (Perez *et al*. 1990). Most of the reviewers agree that this model gives better results (Noorian *et al*. 2008; Padovan and Del Col 2010). The diffuse radiation on the tilted surface in the Perez *et al*. (1990) method is given by:

$$I_{Td} = I_d \left[\begin{array}{l}(1 - F_1) \times (1 + cos(\beta))/20 +\\ F_1 \dfrac{a}{b} + F_2 \times sin(\beta)\end{array}\right] \quad (26)$$

where the coefficients F_1 and F_2 are given by:

$$\begin{aligned}F_1 &= F_{11} + F_{12} \times \Delta + F_{13} \times \theta_Z\\ F_2 &= F_{21} + F_{22} \times \Delta + F_{23} \times \theta_Z\end{aligned} \quad (27)$$

where Δ is the sky brightness and F_{11}, F_{12}, F_{13}, F_{21}, F_{22}, and F_{23} are given in Table 1 as functions of the

Prediction of Hourly Solar Radiation on Horizontal and Inclined Surfaces for Muscat/Oman

Table 1. Coefficients used in Eq. (27) for different sky clearness, ε, categories

ε Category	F_{11}	F_{12}	F_{13}	F_{21}	F_{22}	F_{23}
1	-0.008	0.588	-0.062	-0.06	0.072	-0.022
2	0.13	0.683	-0.151	-0.019	0.066	-0.029
3	0.33	0.487	-0.221	0.055	-0.064	-0.026
4	0.568	0.187	-0.295	0.109	-0.152	-0.014
5	0.873	-0.392	-0.362	0.226	-0.462	0.001
6	1.132	-1.237	-0.412	0.288	-0.823	0.056
7	1.06	-1.6	-0.359	0.264	-1.127	0.131
8	0.678	-0.327	-0.25	0.156	-1.377	0.251

sky clearness index, ε, and the terms a and b are given by:

$$a = max \ (0, \ cos(\theta)) \tag{28}$$

$$b = max \ (0.087, \ cos(\theta_Z)) \tag{29}$$

The sky's brightness, Δ gives an indication about the thickness of the clouds and is given by:

$$\Delta = I_d \ * \ m / I_{eh} \tag{30}$$

where m is the relative optical air mass (Kasten 1966). The sky clearness index, ε, represents the transition from totally overcast sky to a low turbidity clear sky. It is given by:

$$\varepsilon = \frac{\left[\dfrac{(I_d + I_{dn})}{I_d} + 1.041 * \theta_Z^3\right]}{1 + 1.041 * \theta_Z^3} \tag{31}$$

It is used to specify the sky clearness categories which are used in Table 1. The upper and lower bound for each category can be found in Perez *et al.* (1990). For example, a sky clearness index of $\varepsilon = 1$ represents an overcast sky, whereas a sky clearness index of $\varepsilon = 8$ represents a clear sky.

5. Comparison with Measured Data

To validate the model presented in this work, a comparison with hourly measured data from different sources has been conducted. Figures 2 and 3 show comparisons of predictions of the model developed in this work with data from Phoenix, Arizona for June 21st and with those from Seeb Meteorological Center,
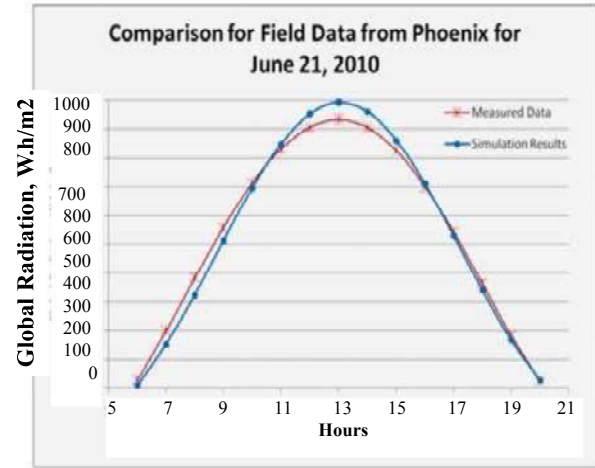
Figure 2. Comparison between predicted and measured hourly global radiation data of Phoenix, Arizona
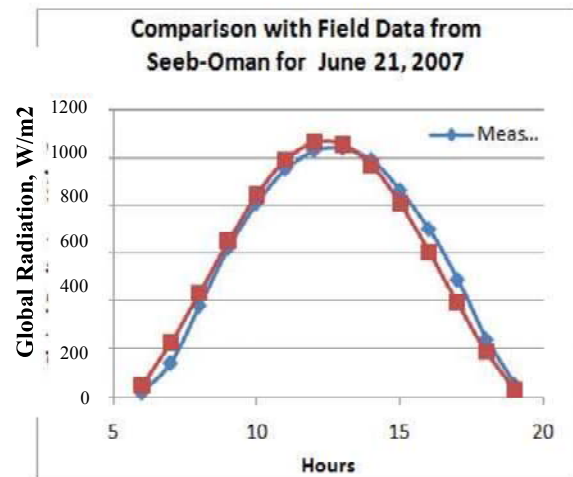
Figure 3. Comparison between predicted and measured hourly global solar radiation data of Seeb/Muscat/Oman

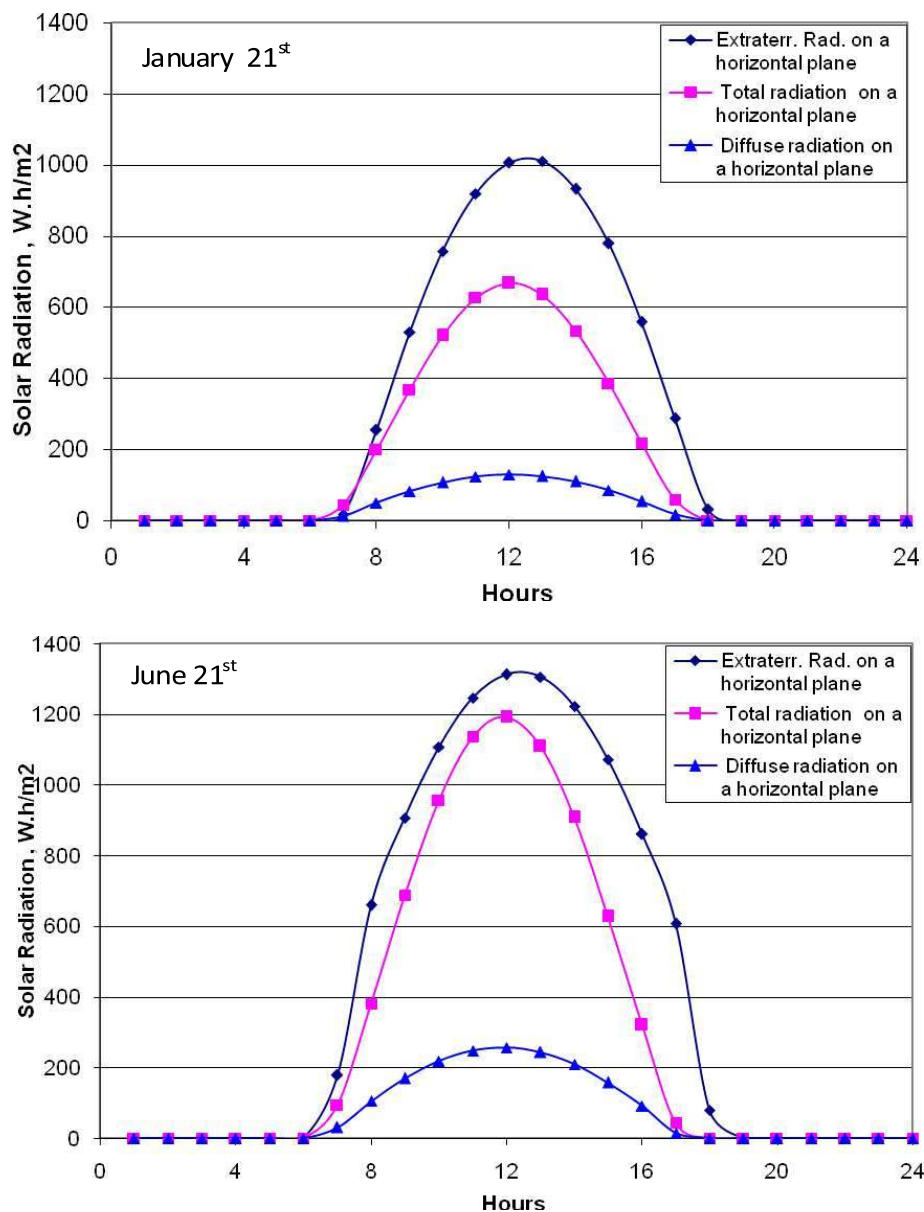*N.Z. Al-Rawahi, Y.H. Zurigat and N.A. Al-Azri*

Figure 4. Terrestrial and extraterrestrial solar radiation in Seeb/Muscat area during January 21st and June 21st

respectively. Clearly, the predictions are in good agreement with the measured data. The maximum difference between predicted and measured data does not exceed 7%. This shows that the model is a reliable tool in predicting hourly solar flux data from measured daily averaged data.

6. Results

Based on the above formulations a computer program has been developed to calculate the hourly solar radiation parameters on horizontal and inclined surfaces. The daily average solar radiation flux data of

Typical Meteorological Year for Seeb/Muscat (Zurigat *et al*. 2003) were used as input. Sample results that show the effect of tilt angle and orientation on the incident solar radiation are presented. In addition, the optimum surface tilt angles and directions for maximum solar radiation collection in Muscat area is deduced. This information is useful when a simple solar collector is to be installed without a tracking system.

Figure 4 shows the hourly extraterrestrial, global, and diffuse radiation on a horizontal surface on January 21st and June 21st. The extraterrestrial and the global radiation increase from January to June by about 30% and 80%, respectively. The increase in the
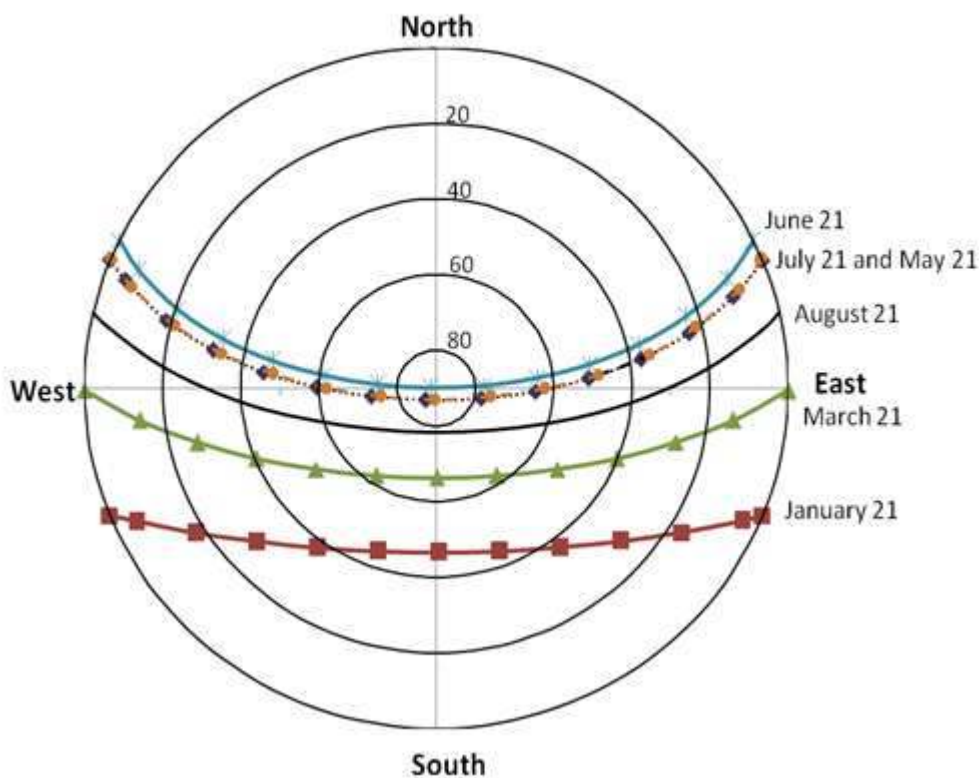
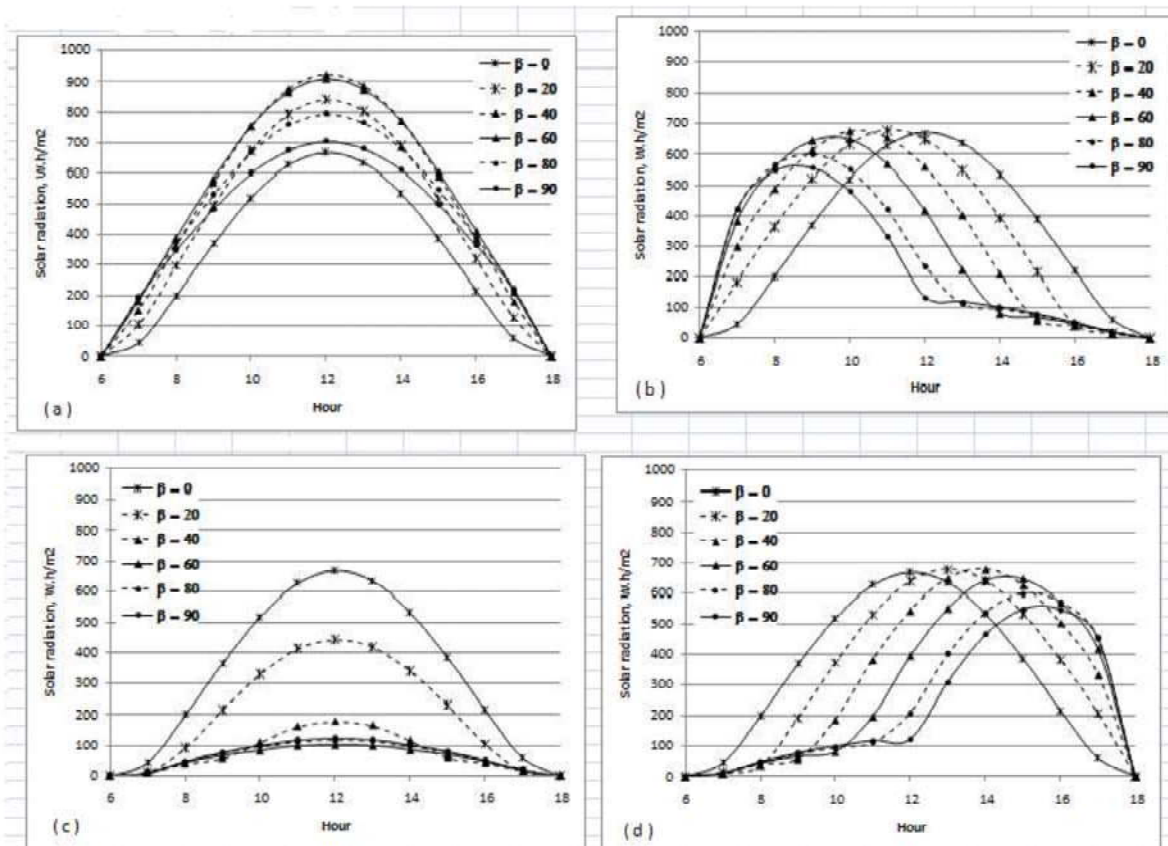**Figure 5.** Sun path diagram for Seeb / Muscat area

Figure 6. Solar radiation in Seeb/Muscat area for planes with different tilt angles, β, towards South (a), East (b), North (c), and West (d) directions for Januatry 21st
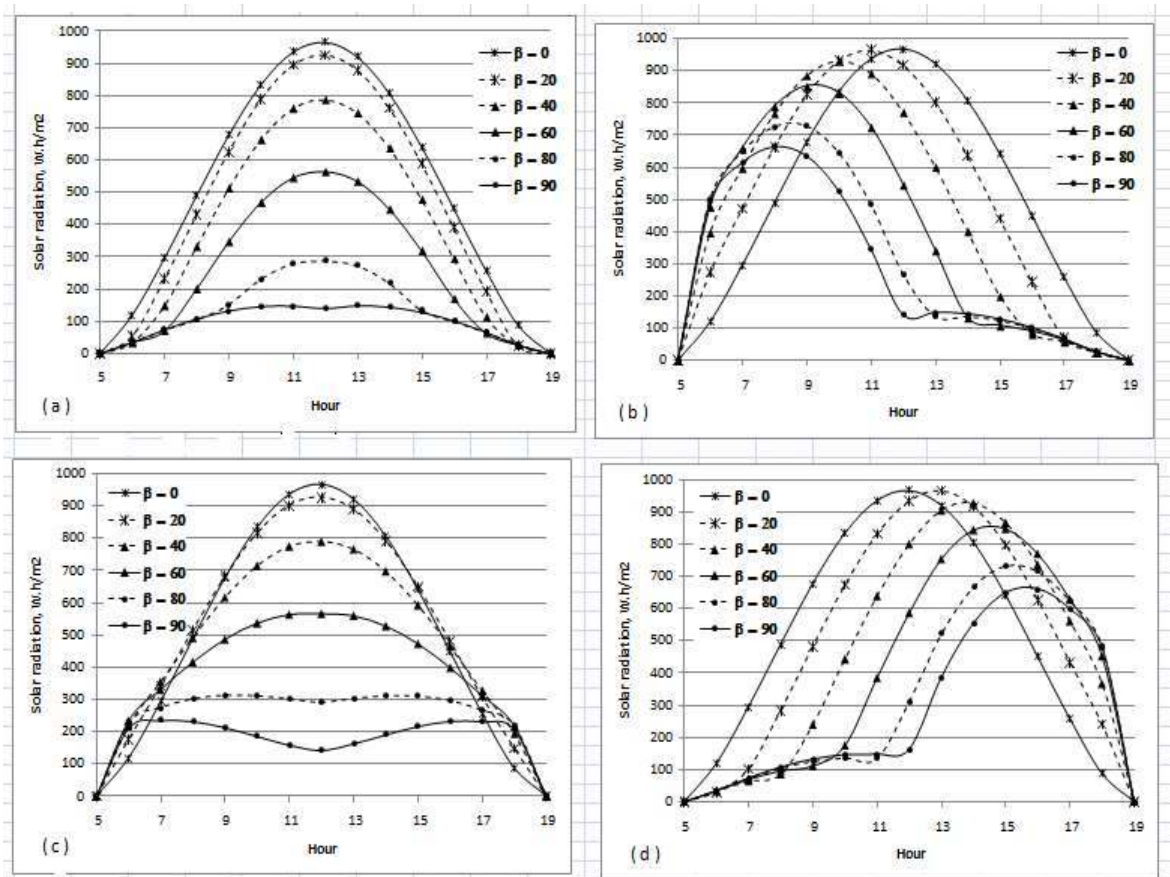
N.Z. Al-Rawahi, Y.H. Zurigat and N.A. Al-Azri

Figure 7. Solar radiation in Seeb/Muscat area for planes with different tilting angles, β, towards South (a), East (b), North (c), and West (d) directions for June 21st

diffuse solar radiation is about 95%. These significant increases in the global and diffuse solar radiation indicate the matching between the availability of solar energy and the need for cooling during hot summer months. Thus, the potential use of solar thermal cooling where it is needed most is obvious.

A number of simulations were carried out to investigate the effect of the tilt angle and the tilt direction. To make sense of the results, the sun path diagram for Seeb/Muscat area is presented in Fig. 5. The diagram shows that the sun is in the southern half of the sky most of the year, especially during the midday period when the solar radiation is at its daily peak. However, the sun is in the northern hemisphere during most of June which represents the hottest month of the year. It can be concluded from the diagram that, for most part of the year, tilting solar collection surfaces towards the south will increase the incident solar radiation on these surfaces. This is clearly illustrated by the results presented in this study.

Figures 6 and 7 show the hourly solar radiation in Seeb/Muscat area for a flat surface at different tilt angles towards South, East, North, and West directions during January 21st and June 21st, respectively. With the exception of surfaces tilted towards the south, the solar radiation on horizontal and tilted surface during

June 21st (see Fig. 7) is greater than that during January 21st. The general trend of the incident solar radiation for surfaces tilted towards the east and the west is almost identical for the two days with higher values for June 21st. On the other hand, as the tilt angle towards the North increases, a higher effect on the hourly solar radiation during January 21st is noticed. It is also noticed that the general trend of the incident solar radiation is almost the same with north-tilted surfaces during January 21st, *i.e.* the solar radiation increases until it reaches a maximum at noon time then it decreases. While tilting surfaces towards the north has less effect on the solar radiation magnitude, the general trend of the solar changes as the tilt angle increases beyond 60º. For larger tilt angles, the increase of the solar radiation levels off before noon and starts to decrease to have a local minimum point at noon. This is clearly understood by looking at the solar path diagram (see Fig. 5). In June, before 12 noon, the sun moves from the northern half to the southern half of the sky which means that the north tilted surfaces will receive less direct solar radiation. The solar radiation on the inclined surface during this period consists of the diffuse solar radiation and the reflected solar radiation only. This shows the importance of having good models for these two components.
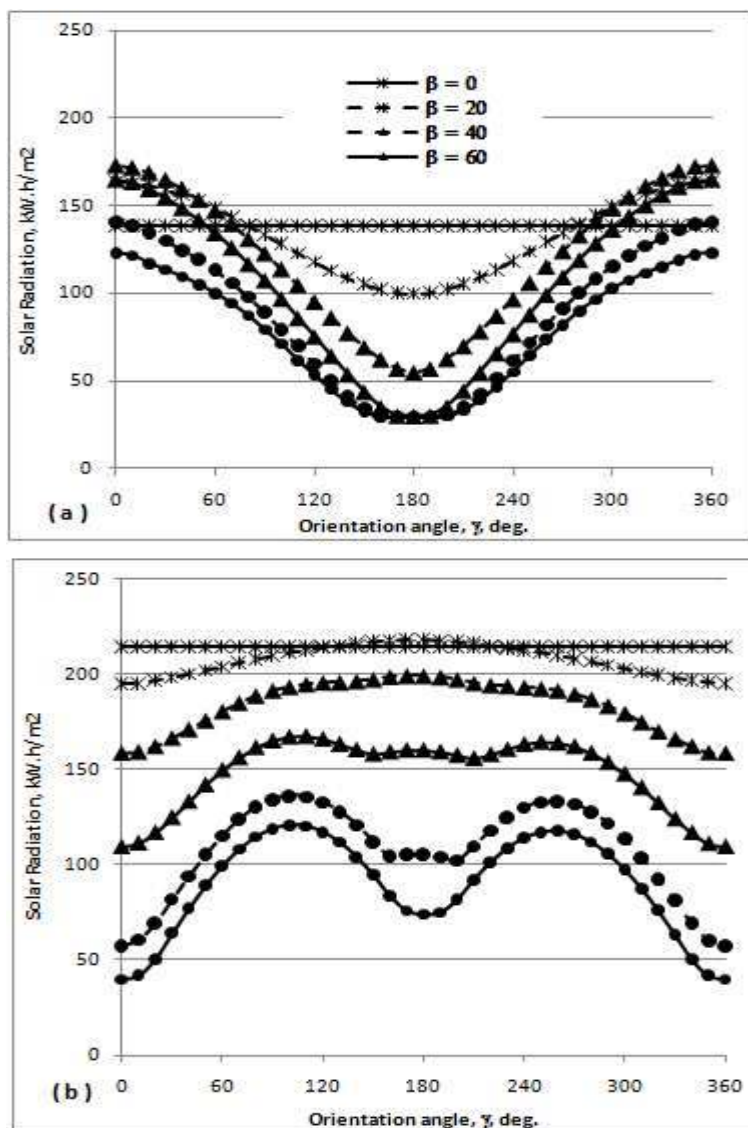
Figure 8. Solar radiation in Seeb/Muscat area for surfaces of different inclination angles, β, as a function of the oriengation angle, γ, for January (a) and June (b). Oriengation angle is measured with $0°$ due South and positive towards East

For south-tilted surfaces, Figs. 6a and 7a show different trends. Compared with June 21st, the solar radiation during January 21st is less sensitive to changes in the tilt angle. The maximum radiation is reached at a tilt angle of 40° at which the received solar radiation increases 40% above that received by a horizontal surface. In June 21st, the received solar radiation decreases significantly as the tilt angle increases. The trends shown in Figs. 6 and 7 indicate that strategies to control the amount of received solar radiation on a surface depend on the surface orientation.

The combined effect of tilt angle and surface orientation on the total incident solar radiation during the months of January and June is shown in Fig. 8. Orientation angles, γ, of 0°, 90°, 180°, and 270° correspond to South, West, North, and East directions, respectively. This figure also shows whether orientations other than the main four (E, W, S, N) have desirable features in terms of received solar radiation. While the figure shows different trends for the two months, there are no special features for other orientations regarding the received solar radiation. During January the minimum received solar radiation is for surfaces tilted towards the North while the maximum received solar radiation is for surfaces tilted towards the South. During the month of June this behaviour is reversed. In January, the maximum received solar radiation is achieved with a tilt angle of about 40° towards the south. During June, the horizontal surface collects more solar radiation than other tilted surfaces
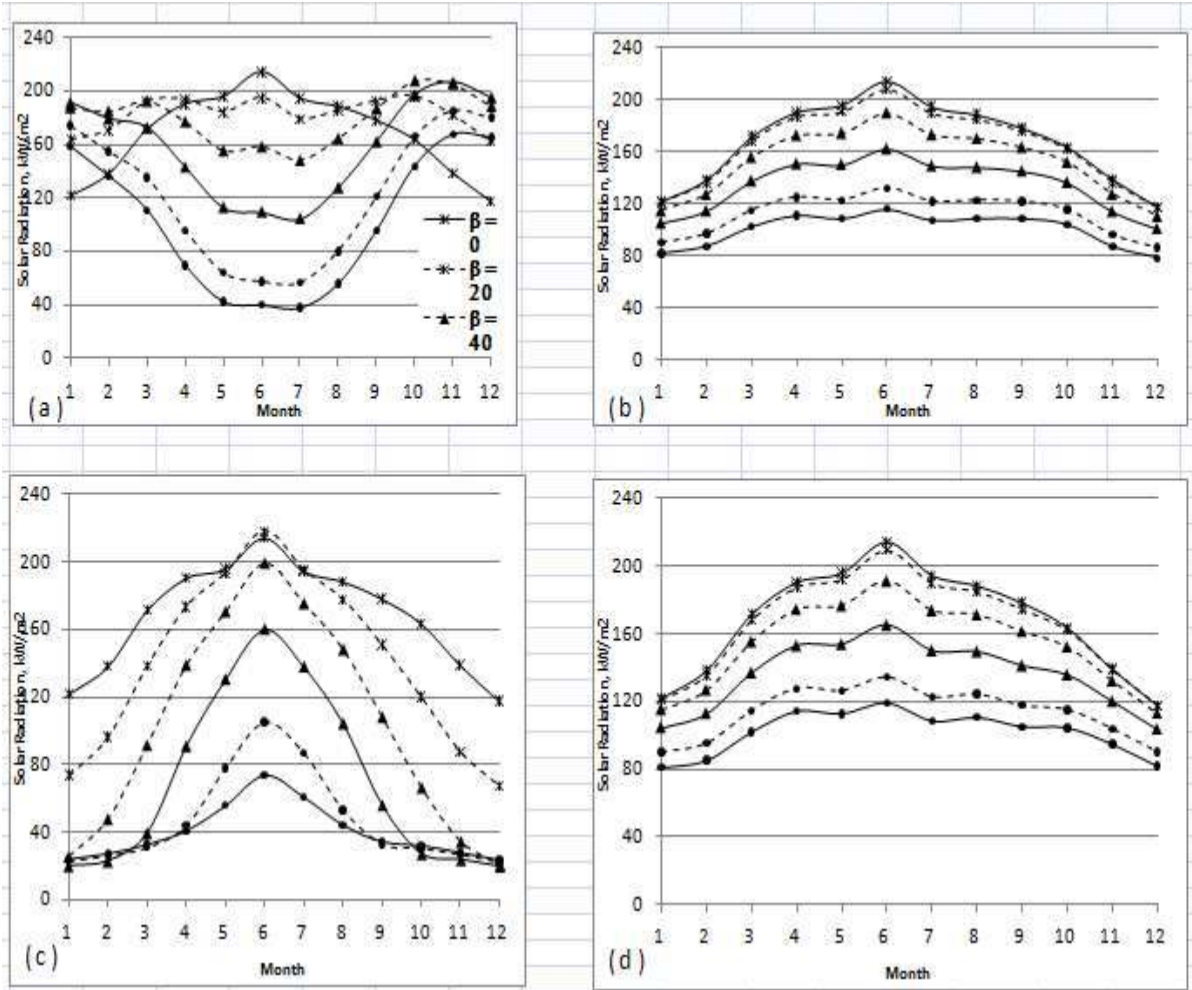
N.Z. Al-Rawahi, Y.H. Zurigat and N.A. Al-Azri

Figure 9. Average monthly incident solar radiation in Seeb/Muscat area for planes with different tilt angles angles, β, toards South (a), East (b), North (c), and West (d) directions, respectively
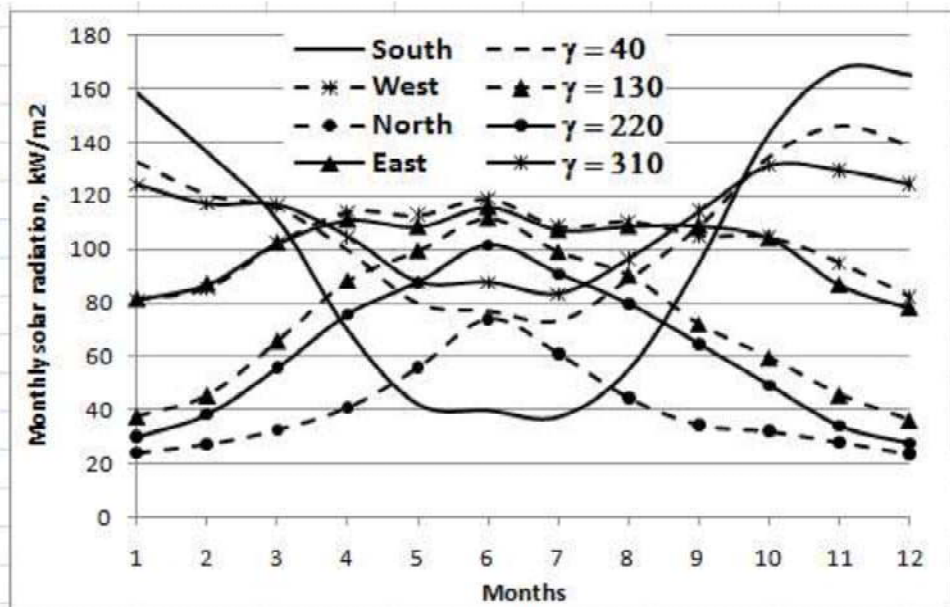

Figure 10. Average monthly solar radiation in Seeb/Muscat area for vertical planes with different orientations. Orientation angle is measured with 0° due South and positive towards East

Prediction of Hourly Solar Radiation on Horizontal and Inclined Surfaces for Muscat/Oman

Table 2a. Summary of incident solar energy for tilted surfaces for the months of January through June using the model of (Perez *et al.* 1990)

Month		1	2	3	4	5	6
$I_{H, Ave.}$, kW.h/m^2/day		3.93	4.94	5.53	6.35	6.32	7.14
$I_{T, Max.}$, kW.h/m^2/day		6.21	6.63	6.29	6.50	6.37	7.31
Direction for $I_{T, Max.}$		South	South	South	South	North	North
Tilting angle for $I_{T, Max.}$ (1% difference range of angles)		55° (45° – 60°)	45° (40° – 50°)	30° (25° – 35°)	15° (5° – 20°)	10° (0° – 15°)	15° (5° – 20°)
Solar radiation on a vertical surface, kW.h/m^2/day	South	5.11	4.86	3.58	2.32	1.37	1.33
	West	2.62	3.05	3.29	3.81	3.64	3.97
	North	0.78	0.97	1.05	1.36	1.80	2.47
	East	2.63	3.11	3.31	3.71	3.51	3.87

Table 2b. Summary of incident solar energy for tilted surfaces for the months July through December using the model of (Perez *et al.* 1990)

Month		7	8	9	10	11	12
$I_{H, Ave.}$, kW.h/m^2		6.27	6.08	5.94	5.28	4.63	3.79
$I_{T, Max.}$, kW.h/m^2		6.37	6.12	6.44	6.70	6.97	6.32
Direction for $I_{T, Max.}$		North	South	South	South	South	South
Tilt angle for $I_{T, Max.}$ (1% difference range of angles)		10° (5° – 15°)	10° (0° – 15°)	25° (20° – 30°)	40° (35° – 45°)	50° (45° – 65°)	55° (45° – 60°)
Solar radiation on a vertical surface, kW.h/m^2/day	South	1.22	1.79	3.18	4.64	5.59	5.33
	West	3.50	3.57	3.51	3.37	3.16	2.64
	North	1.96	1.43	1.15	1.03	0.93	0.76
	East	3.46	3.51	3.63	3.36	2.89	2.52

except for surfaces with a tilt angle of 20° towards the north where the received solar radiation is slightly higher. It should be noted that the results presented here assume that the surrounding diffuse reflectance is isotropic, *i.e.* the same in all directions (Dry bare ground of ρ_r = 0.2).

Looking at the broader picture, Fig. 9 shows the incident solar radiation on tilted surfaces for the whole year. As noticed previously, surfaces tilted towards the East and the West have similar trends and the trend is almost the same for other tilt angles. For surfaces tilted towards the South, in the period between October to March, the effect of tilt angle on the received solar radiation is relatively small. However, the tilt angle has more significant effect between April and September. For surfaces tilted towards the North the received solar radiation is sensitive to the tilt angle throughout the year.

Vertical surfaces (β = 90°) require further attention as they represent the major part of the building envelop which contributes significantly to the cooling/heating loads. Figure 10 shows the received solar radiation for vertical surfaces at different compass orientations. During summer the West- and East-facing vertical surfaces receive higher solar radiation than the South- and

North-facing ones. These results explain why the orientation of buildings in Muscat area should be East-West with the longest vertical surface facing south. During summer time, this orientation minimizes the solar gain and consequently, the cooling load. It is noticed also that South-facing vertical surfaces receive more solar radiation than North-facing ones for most part of the year and the difference is considerably large.

Tables 2a and 2b present quite useful information regarding solar radiation in Seeb/Muscat area. For each month it shows the average solar radiation on horizontal surfaces, the tilt angle that results in maximum received solar radiation and the corresponding solar radiation, the range of tilt angles that will maintain the received solar radiation within 1% from the maximum value, and the solar radiation on vertical surfaces in the four main directions. The information about the received solar radiation on horizontal and vertical surfaces can be quite useful in estimating the building heat gain. Also, the information about the maximum received solar radiation and the tilt angle are useful for sun tracking solar collectors that are manually adjusted every month or so. One of the general rules of thumb in solar radiation is that during
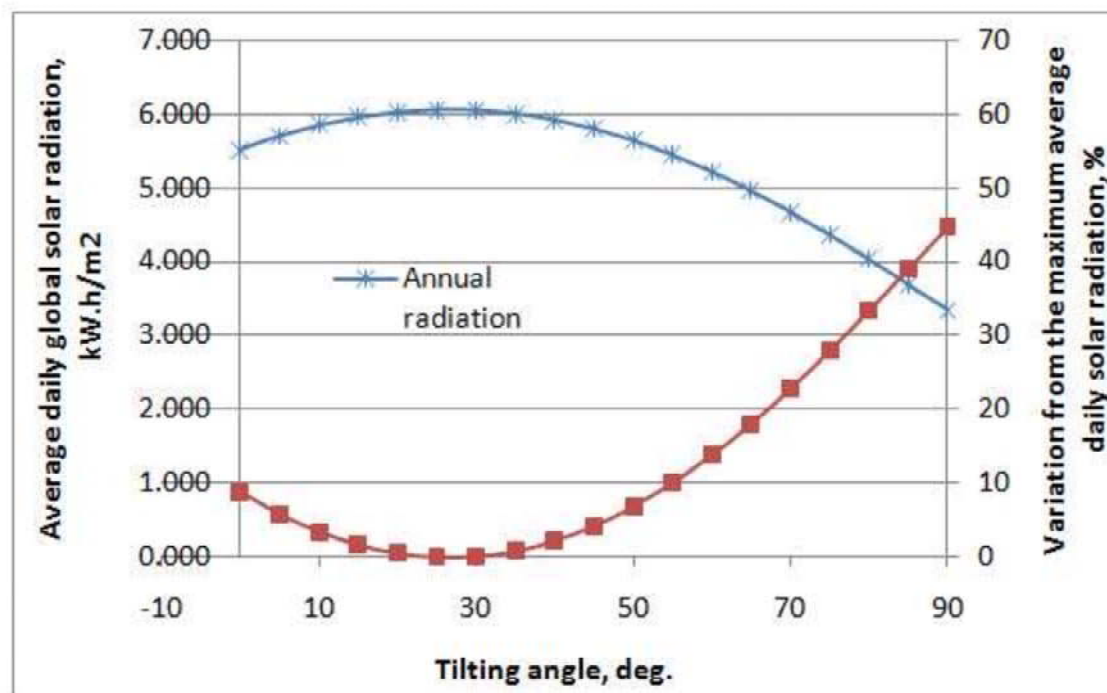
Figure 11. Average daily incident solar radiation energy in Seeb / Muscat area for different tilt angles

summer the tilt angle that will give the maximum received solar radiation equals the location latitude minus 15º. The presented data is in agreement with this rule since the latitude of Seeb/Muscat area is 23.35º. Another rule of thumb is that during winter time the tilt angle that will give the maximum received solar radiation equals the location latitude plus 15º. This again is in agreement with the presented range of tilt angle for maximum received solar radiation.

Figure 11 shows the average received solar radiation if the tilt angle is kept the same throughout the year. When the tilt angle of a solar collector is fixed, a tilt angle of about 25º will receive the maximum solar radiation. Figure 11 also shows the resulting reduction in the incident solar radiation, in percentage, as a function of tilt angle. For example, using a fixed horizontal surface ($\beta = 90º$) will result in about 10% reduction in total solar radiation incident on that surface.

Conclusions

In this paper, prediction of hourly terrestrial solar radiation on a horizontal surface: direct beam, diffuse and global from measured daily averaged global solar radiation on the same surface has been conducted. The same parameters were also modelled for inclined surfaces. Thus, an important tool for building and solar thermal systems design, simulations, and performance assessments has been developed. The predicted hourly solar radiation incident on a horizontal surface was compared with hourly data measured locally at Seeb Meteorological Centre as well as elsewhere outside Oman.

The effect of tilt angle and orientation on the incident solar radiation fluxes are presented along with optimum surface tilt angles and directions for maximum solar radiation collection in Muscat area. This information is useful when a simple solar collector is to be installed without a tracking system. In general, surfaces tilted towards the East and the West have similar trends and the trend is almost the same for other tilt angles. For surfaces tilted towards the South, in the period between October to March, the effect of tilt angle on the received solar radiation is relatively small. However, the tilt angle has more significant effect between April and September. For surfaces tilted towards the North the received solar radiation is sensitive to the tilt angle throughout the year.

During summer the West- and East-facing vertical surfaces receive higher solar radiation than the South- and North-facing ones. These results explain why the orientation of buildings in Muscat area should be East-West with the longest vertical surface facing south. In addition, a table that presents important monthly solar radiation information for horizontal, inclined and vertical surfaces has been presented. Assuming isotropic reflection of diffuse radiation, the results show that for January the maximum received solar radiation is

achieved with tilt angle of about 40⁰ towards the south. For June, the horizontal surface collects more solar radiation than other tilted surfaces except for surfaces with a tilt angle of 20⁰ towards the north where the received solar radiation is slightly higher. It is believed that the results presented in Tables 2a and 2b are quite useful for quick estimation of solar radiation for calculations of cooling load and solar collector performance.

Acknowledgments

References

Al-Hinai AH, Al-Alawi SM (1995), Typical solar radiation data for Oman. Applied Energy 52:153-163

ASHRAE handbook (1999), HVAC applications, Atlanta (GA): ASHRAE.

Collares-Pereira M, Rabl A (1979), The average distribution of solar radiation - correlations between diffuse and hemispherical and between daily and hourly insolation values. Solar Energy 22:155-164.

Duffie JA, Beckman WA (1980), Solar engineering of thermal processes. John Wiley, New York.

Gueymard C (1993), Critical analysis and performance assessment of clear-sky solar irradiance models using Theoretical and Measured Data. Solar Energy 51(2):121-138.

Iqbal M (1978), Estimation of the monthly average of the diffuse component of total insolation on a horizontal surface. Solar Energy 20(1):101-105.

Kasten A (1966), A new table and approximate formula for relative optical air mass. Arch. Meteorol Geophys. Bioklimatol Ser. B 14:206-223.

Lam JC, Li DHW (1996), Correlation between global solar radiation and its direct and diffuse components. Building and Environment 31(6):527-535.

Liu BYH, Jordan RC (1962), Daily insolation on surfaces tilted towards the equator. Trans ASHRAE 67:526-541.

Mellit A, Eleuch H, Benghanem M, Elaoun C, Massi Pavan A (2010), An adaptive model for predicting of global, direct and diffuse hourly solar irradiance. Energy Conversion and Management 51:771-782.

Nijmeh S, Mamlook R (2000), Testing of two models for computing global solar radiation on tilted surfaces. Renewable Energy 20(1):75-81.

Noorian AM, Moradi M, Kamali GA (2008), Evaluation of 12 models to estimate hourly diffuse irradiation on inclined surfaces. Renewable energy 33(6):1406-1412.

Notton G, Muselli M, Louche A (1996), Two estimation methods for monthly mean hourly total irradiation on tilted surfaces from monthly mean daily horizontal irradiation from solar radiation data of ajaccio, corsica. Solar Energy 57(2):141-153.

Padovan A, Del Col D (2010), Measurement and modeling of solar irradiance components on horizontal and tilted planes. Solar Energy 84:2068-2084.

Perez R, Ineichen P, Seals R, Michalsky J, Stewart R (1990), Modelling daylight availability and irradiance components from direct and global irradiance. Solar Energy 44:271-289.

Tymvios FS, Jacovides CP, Michaelides SC, Scouteli C (2005), Comparative study of angstrom's and artificial neural networks methodologies in estimating global solar radiation. Solar Energy 78:752-762.

Ulgen K, Hepbasli A (2009), Diffuse solar radiation estimation models for turkey's big cities. Energy Conversion and Management 50:149-156.

Zervas PL, Sarimveis H, Palyvos JA, Markatos NCG (2008), Prediction of daily global solar irradiance on horizontal surfaces based on neural-network techniques. Renewable Energy 33:1796-1803.

Zurigat YH, Sawaqed N, Al-Hinai H, Jubran B (2003), Development of typical meteorological years for different climatic regions in Oman, Final Report, Petroleum Development Oman.